

Passive imaging and emissivity measurement with a 4 K-cryocooled terahertz photoconductive detector

Makoto Aoki¹, Saroj R. Tripathi², Masanori Takeda¹,
and Norihisa Hiromoto^{1a)}

¹ Graduate School of Science and Technology, Shizuoka University
3–5–1 Johoku, Naka-ku, Hamamatsu, Shizuoka 432–8011, Japan

² Present address is Eco Topia Science Institute, Nagoya University
Furo-cho, Chikusa-ku, Nagoya, Aichi 464–8603, Japan

a) dnhhirom@ipc.shizuoka.ac.jp

Abstract: We have demonstrated terahertz (THz) passive imaging of room-temperature objects using a 4 K-cryocooled THz photoconductive detector with background limited infrared performance (BLIP) at around 1.5–2.5 THz. Images of a safety razor blade and a coin concealed in a plastic package or an envelope are successfully obtained with spatial resolutions of wavelength order using the THz passive imaging system. We have compared the measured THz intensity of several materials with emissivities calculated using the reported optical constants. The result shows that the THz intensity has a good linear relation to the emissivity, which means THz emissivity of an unknown material can be estimated at a room-temperature with the THz passive imaging system.

Keywords: terahertz, passive imaging, sensing, emissivity, detector

Classification: Sensing hardware

References

- [1] K. Sakai, *Terahertz Optoelectronics*, New York, Springer-Verlag, Berlin Heidelberg, 2005.
- [2] R. Köhler, A. Tredicucci, F. Beltram, H. E. Beere, E. H. Linfield, A. G. Davies, D. A. Ritchie, R. C. Iotti, and F. Rossi, “Terahertz semiconductor - heterostructure laser,” *Nature*, vol. 417, pp. 156–159, May 2002.
- [3] D. M. Mittleman, M. Gupta, R. Neelamani, R. G. Baraniuk, J. V. Rudd, and M. Koch, “Recent advances in terahertz imaging,” *Appl. Phys. B: Laser Opt.*, vol. 68, no. 6, pp. 1085–1094, April 1999.
- [4] M. Usami, T. Iwamoto, R. Fukasawa, M. Tani, M. Watanabe, and K. Sakai, “Development of a THz spectroscopic imaging system,” *Phys. Med. Biol.*, vol. 47, no. 21, pp. 3749–3753, Oct. 2002.
- [5] S. P. Mickan and X.-C. Zhang, “T-ray sensing and imaging,” *Int. J. High*

- Speed Electron. Syst.*, vol. 13, no. 2, pp. 601–676, June 2003.
- [6] P. H. Siegel and R. Dengler, “Terahertz heterodyne imaging Part I: Instruments,” *Int. J. Infrared Millimeter Waves*, vol. 27, no. 4, pp. 456–480, April 2006.
- [7] G. Gaussorgues, *Infrared Thermography*, London, Chapman and Hall, 1994.
- [8] L. Yujiri, M. Shoucri, and P. Moffa, “Passive millimeter-wave imaging,” *IEEE Microw. Mag.*, vol. 4, no. 3, pp. 39–50, Sept. 2003.
- [9] N. Hiromoto, T. Itabe, H. Shibai, H. Matsuhara, T. Nakagawa, and H. Okuda, “Three-element stressed Ge:Ga photoconductor array for the infrared telescope in space,” *Appl. Opt.*, vol. 31, no. 4, pp. 460–465, Feb. 1992.
- [10] M. A. Ordal, R. J. Bell, R. W. Alexander, Jr., L. L. Long, and M. R. Querry, “Optical properties of Au, Ni, and Pb at submillimeter wavelengths,” *Appl. Opt.*, vol. 26, no. 4, pp. 744–752, Feb. 1987.
- [11] L. Thrane, R. H. Jacobsen, P. U. Jepsen, and S. R. Keiding, “THz reflection spectroscopy of liquid water,” *Chem. Phys. Lett.*, vol. 240, no. 4, pp. 330–333, June 1995.

1 Introduction

The innovative development in terahertz (THz) technology including the THz time-domain spectroscopy (TDS) (reviewed in [1]) and the THz quantum cascade laser (QCL) [2] has recently brought large attention in THz imaging as an intensive method of non-destructive inspection for security and industry applications. Advantage of the THz imaging comes from the characteristics of THz waves such as transmitting many nonmetallic materials without ionization, high spatial resolution compared with microwave and detection of various materials including organic and bio-materials through specific absorption spectra (e.g. [3, 4, 5]).

THz imaging technique can be classified into active and passive methods. The former detects transmitted or reflected radiation from a sample using an external THz source and the latter observes thermal radiation emitted from a sample. Passive imaging has a great advantage that it needs no expensive source in THz region. However, it requires sensitive THz detectors such as cryogenic detectors or heterodyne mixers [6] to receive weak thermal THz radiation from 300 K blackbody radiation. Therefore, studies on the THz passive imaging of room-temperature objects have been rare so far in comparison with the THz active imaging and the passive imaging in infrared region such as thermography [7] and in millimeter wavelengths for security applications [8].

We have developed a THz detector system which employs four THz photoconductive detectors to cover a response in wide frequency ranges from 0.8 to 4.0 THz and a mechanical 4 K-GM-cryocooler instead of a liquid helium container in order to perform convenient use for practical THz applications. Our detector system has the background limited performance under the 300 K background radiation by adopting sensitive THz photoconductors and sup-

pressing the vibration noise of cryocooler.

In this study, we demonstrate the potential and advantage of THz passive imaging using the 4 K-cryocooled THz photoconductive detector system.

2 THz passive imaging: Instrument and measurement

In the passive imaging at THz region, we have to detect weak thermal radiation from a sample which is much smaller than the peak intensity of 300 K blackbody radiation at about 30 THz, and moreover, surrounding objects emit the similar thermal radiation. In our passive imaging system, we used a stressed Ge:Ga photoconductor [9] with high detectivity cooled at 4 K to measure the small difference in THz radiation between a sample and surroundings. The stressed Ge:Ga detector has the background limited infrared performance (BLIP) in 1.5 to 2.5 THz frequency region, a responsivity of 48 A/W (4.8×10^7 V/W) and a noise equivalent power (NEP) of about 10^{-14} W/ $\sqrt{\text{Hz}}$ at 4 K. The detector assembly comprises a stressing mount containing a detector chip, a Winston cone condenser, THz filters and a 200 μm pinhole placed in front of the condenser. The passive imaging system also consists of two off-axis parabolic mirrors, and a raster scan stage to hold samples, as shown in Fig. 1. THz wave emitted from the sample is collected and collimated with the first off-axis parabolic mirror and is focused on the pinhole using the second off-axis parabolic mirror. The optical length traveling in air is 300 mm. The THz wave goes into the Winston cone through the pinhole and then condensed onto the stressed Ge:Ga detector. A sample is moved in a plane perpendicular to the optical axis using the X-Y raster scan stage and a passive image of $50 \times 50 \text{ mm}^2$ is obtained with 500 μm -step measurement in 15 minutes by scanning at a speed of 10 mm/s.

We have evaluated a spatial resolution of the imaging system with the 200 μm pinhole using a knife edge method and proved the resolution of 240 μm

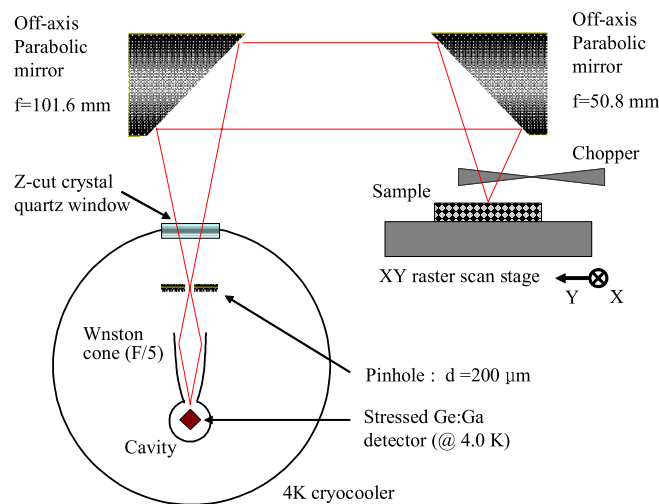


Fig. 1. Schematic configuration of the THz passive imaging system using 4 K-cryocooled sensitive THz photoconductive detector system.

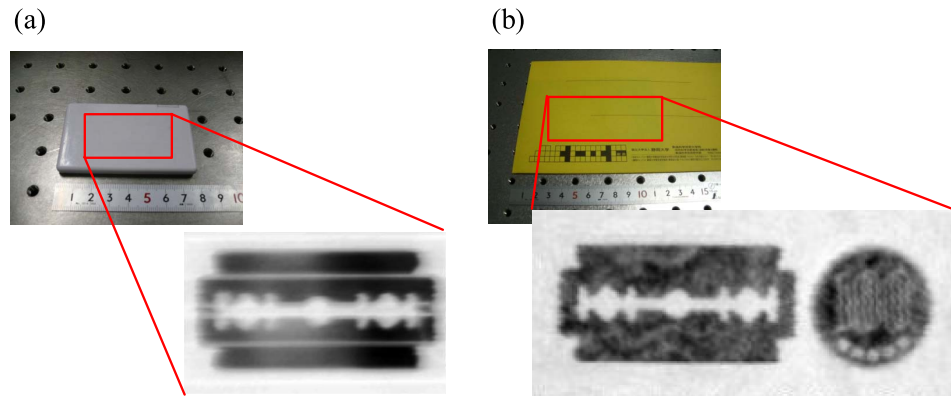


Fig. 2. THz passive imaging of (a) Safety razor blade concealed in the plastic package, and (b) Safety razor blade and 100 yen coin concealed in the envelope.

which is nearly limited by diffraction at 1.5–2.5 THz of the stressed Ge:Ga detector’s spectral response. The measured noise-voltage-density of our system is $1.4 \times 10^{-7} \text{ V}/\sqrt{\text{Hz}}$ at the detector temperature of 4 K, which is consistent with the theoretical value limited by the photon noise and proves the BLIP performance. The NEP of our system is $7.7 \times 10^{-15} \text{ W}/\sqrt{\text{Hz}}$ and the noise equivalent temperature difference (NETD) corresponds to 11 mK.

We have demonstrated to take THz passive images of a safety razor blade and a 100 yen coin concealed in a plastic package and an envelope as shown in Fig. 2(a) and (b) which is obtained by scanning $50 \times 25 \text{ mm}^2$ and $75 \times 35 \text{ mm}^2$ with the measurement resolution of 500 and $250 \mu\text{m}$, respectively. The acquisition time to take the image is about 10 min for Fig. 2(a) and 40 min for Fig. 2(b). These passive images are observed small changes in the emission and reflection of thermal radiation from the room-temperature objects. Therefore, the uneven surface structures of the concealed metal and the emissivity difference between metals and concealing materials can be seen as variations in the THz intensity with high spatial resolution. It should be noted that the thickness change of the plastic package and the non-uniformity of the envelope paper are also seen as the shadings on the metal surface. In addition, the surface pattern of the coin is identified by changes in emissivity and reflectivity due to concavity and convexity of the metal surface.

3 Emissivity measurement

We suggest that the emissivity (ε) of samples can be estimated from the output signal (V) of THz passive imaging because the THz intensity is proportional to the product of emissivity and blackbody radiation and has a linear dependence on the emissivity if the temperature of samples is constant.

It is necessary to perform the calibration of the THz imaging system by measuring at least two samples with known emissivity for estimating the emissivity of an unknown material. We have measured the THz intensity of several materials at a room temperature ($300.2 \pm 0.4 \text{ K}$). Measured samples are a gold mirror, high resistivity silicon, Z-cut crystal quartz, Acrylic sheet,

acrylonitrile butadiene styrene (ABS) sheet, Teflon sheet and pure water. The emissivity is equal to absorptance A , and expressed as $\varepsilon = A = 1 - \exp(-\alpha d)$ by using Kirchhoff's law and Lambert-Beer law. Where α and d are the absorption coefficient and the thickness of a sample. We adopted the absorption coefficient α reported in the literatures (e.g. $\varepsilon = 0.004$ for gold [10] and $\varepsilon = 0.837$ for pure water [11]) or measured with a THz-TDS by ourselves, which is the value at around 2 THz and weighted by the spectral sensitivity of the stressed Ge:Ga detector. The calculated emissivity is compared with THz intensity measured using the passive imaging system and shown in Fig. 3 (a).

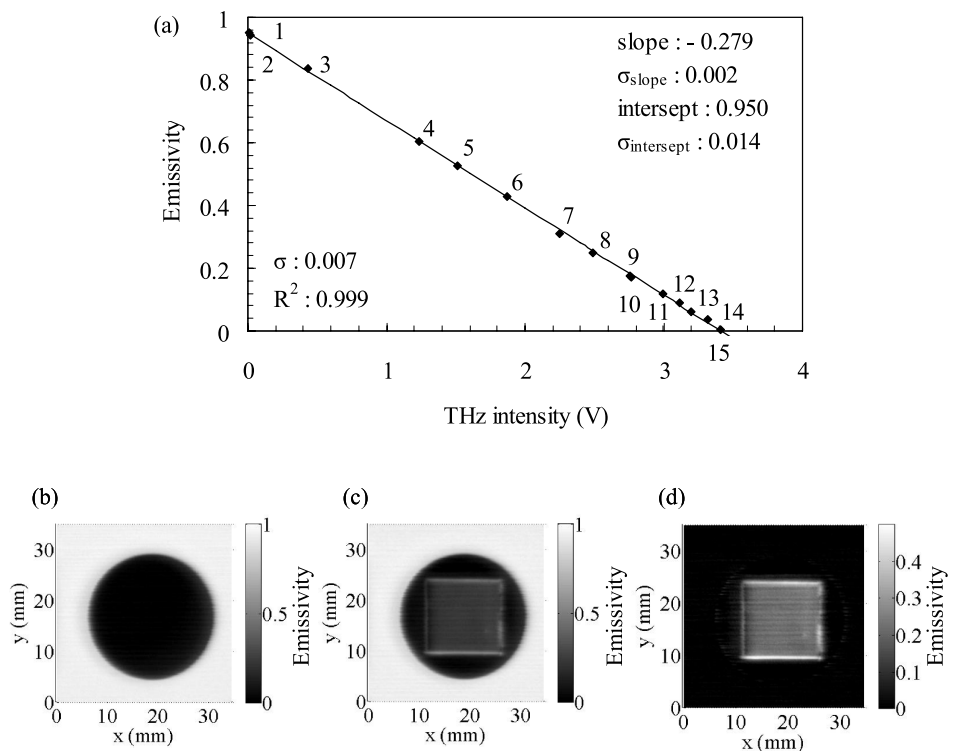


Fig. 3. (a) Calculated emissivity vs. THz intensity measured with the passive imaging system for 15 samples and the least square fitting line derived from the data. The fitting line is expressed as $\varepsilon = -0.279 V + 0.950$ with σ_{slope} of 0.002 and $\sigma_{\text{intercept}}$ of 0.014. Standard deviation (σ) around the fitting line and determination coefficient (R^2) is 0.007 and 0.999, respectively. Mark 1 shows 2 mm-thick acrylic sheet. Mark 2 shows 2 mm-thick ABS sheet. Mark 3 shows pure water. Mark 4, 5, 6, 7, 10, 12 and 14 show 5, 4, 3, 2, 1, 0.5 and 0.2 mm-thick Teflon, respectively. Mark 8 shows 3 mm-thick z-cut crystal quartz. Mark 9, 11 and 13 shows 3, 2 and 1 mm-thick high resistivity silicon, respectively. Mark 15 shows gold mirror.

Emissivity imaging of (b) Gold mirror, (c) Polyethylene sheet on the gold mirror, and (d) Difference between Fig. 3 (b) and (c).

Figure 3(a) also displays a calibration line derived using the linear least-squares method to the data, which is $\varepsilon = -0.279V + 0.950$. The standard deviation around the fitting line ($\sigma = 0.007$) and the determination coefficient of $R^2 = 0.999$, and the standard deviations in slope and interception of the fitting line are derived and inserted in Fig 3(a). These results show the emissivity (ε) can be estimated from the THz intensity (V) using the relation between them with an accuracy less than 10^{-2} of the standard deviation in ε .

To validate the method to estimate the emissivity in imaging, we took THz images of a Gold mirror and a 2 mm-thick polyethylene (PE) sheet with an area of $15 \times 15 \text{ mm}^2$ on the Gold mirror, and derived their emissivity images using the relation between ε and V in Fig. 3(b) and Fig. 3(c), respectively. Figure 3(b) shows that the emissivity of the Gold mirror is low and Figure 3(c) displays that the PE sheet emits a small thermal emission due to its emissivity larger than that of the Gold mirror. From Fig. 3(b) and Fig. 3(c), we computed a difference emissivity image between the PE sheet plus the Gold mirror and the Gold mirror only. The difference image has to be only the emissivity image of the PE sheet, which is shown in Fig. 3(d). Although the apparent emissivity increases at the edges of the PE sheet due to extra THz emission from the surroundings by reflection and scattering, the emissivity is almost constant on the flat surface of the PE sheet, which is derived as 0.227 ± 0.002 . To confirm the measured result, we have calculated the emissivity of PE sheet from the absorption coefficient and its thickness. We adopted the absorption coefficient α of 1.3 cm^{-1} measured with the THz-TDS, which is the value at around 2 THz weighted by the spectral sensitivity of the stressed Ge:Ga detector. The calculated emissivity ε is 0.229, which is in good accordance with the measured value.

4 Summary

We have obtained the THz passive images of room-temperature objects concealed in the plastic package and envelope at 1.5–2.5 THz using a 4 K-cryocooled THz photoconductive detector with BLIP. The calibration line between the THz intensity and emissivity calculated from reported optical constants of materials are determined using the measurement of several samples with the THz passive imaging system, because the emissivity is proportional to the THz intensity if the samples have the same temperature. We have obtained the emissivity images of several materials using the THz intensity images and the calibration line. The THz passive imaging with sensitive THz detectors has the potential and advantage in the application to the nondestructive inspection and the quantitative evaluation of emissivity of unknown objects.